The time-optimal trajectories for an omni-directional vehicle

Devin J. Balkcom and Paritosh A. Kavathekar
Department of Computer Science
Dartmouth College
Hanover, NH 03755
{devin, paritosh}@cs.dartmouth.edu

Matthew T. Mason
Robotics Institute
Carnegie Mellon University
Pittsburgh, PA 15213
matt.mason@cs.cmu.edu

Abstract

A common mobile robot design consists of three 'omni-wheels' arranged at the vertices of an equilateral triangle, with wheel axles aligned with the rays from the center of the triangle to each wheel. Omniwheels, like standard wheels, are driven by the motors in a direction perpendicular to the wheel axle, but unlike standard wheels, can slip in a direction parallel to the axle. Unlike a steered car, a vehicle with this design can move in any direction without needing to rotate first, and can spin as it does so.

The *shortest* paths for this vehicle are straight lines. However, the vehicle can move more quickly in some directions than in others. What are the fastest trajectories? We consider a kinematic model of the vehicle and place independent bounds on the speeds of the wheels, but do not consider dynamics or bound accelerations. We derive the analytical *fastest* trajectories between configurations. The time-optimal trajectories contain only spins in place, circular arcs, and straight lines parallel to the wheel axles. We classify optimal trajectories by the order and type of the segments; there are four such classes, and there are no more than 18 control switches in any optimal trajectory.

1 Introduction

This paper presents the time-optimal trajectories for a simple model of the common mobile-robot design shown in figure 1(b). The three wheels are "omni-wheels"; the wheels not only rotate forwards and backwards when driven by the motors, but can also slip sideways freely. Such a robot can drive in any direction instantaneously.

(a) Photograph.   (b) Notation.
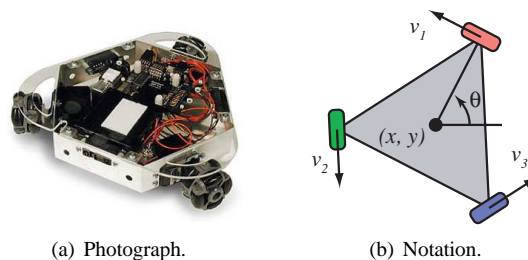
Figure 1: The Palm-Pilot Robot Kit, an example of an omni-directional vehicle. Photograph used by permission of Acroname, Inc., www.acroname.com.

The only other ground vehicles for which the fastest trajectories are known explicitly are the steered cars studied by Dubins [6] and by Reeds and Shepp [9] and differential-drives [1]. Although our results are specific to the particular vehicle studied, we hope that expanding the set of vehicles for which the optimal trajectories are known will eventually lead to a more unified understanding of the relationship between robot mechanism design and the use of resources.

We take a simple kinematic model of the robot – the configuration is $(x, y, \theta) \in \mathbf{SE}^2$, and the controls v_1, v_2, and v_3 are the velocities of the wheels perpendicular to the axles, as shown in figure 1(b). We assume independent bounds on the speeds of the wheels; $v_{\{1,2,3\}} \in [-1, 1]$.

We show that the time-optimal trajectories between any pair of configurations consist of spins in place, circular arcs, and straight lines parallel to the wheel axles. We label each segment type by a letter: P, C, S, respectively. There are specific sequences of segments that may be op-

<center>1</center>

timal; we call the four classes of trajectories *spin*, *roll*, *shuffle*, and *tangent*.

1. *Spin* trajectories consist of a spin in place through an angle no greater than π, and are described by the single-letter control sequence P. Figure 3(a) shows an example.

2. *Roll* trajectories consist of a sequence of circular arcs of equal radius separated by spins in place. Figure 4(a) shows an example. The trajectories are periodic; a single period is of the form CPCPC. The centers of the arcs all fall on the same line. With the possible exception of the first and last segments, the arcs all encompass the same angle, as do the spins, and the sum of the angular displacement of a complete arc and a complete spin is $120°$. There are no more than four circular arcs in any optimal trajectory.

3. *Shuffle* trajectories are composed of repetitions of sequences of three circular arcs followed by a spin, CCCP, and contain no more than seven control switches. Figure 4(b) shows an example. A complete period of a *shuffle* moves the vehicle 'sideways' in a direction parallel to a line connecting two wheels.

4. *Tangent* trajectories consist of a sequence of arcs of circles and spins in place separated by arbitrarily long translations in a direction parallel to the line containing the center of the robot and one of its wheels; see figure 4(c). All straight segments are co-linear. The control sequence is CSCSCP . . ., and trajectories contain no more than 18 switches. Intuitively, the robot 'lines up' in its fastest direction of translation, translates, and then follows arcs of circles to arrive at its final position and orientation.

Why study optimal trajectories? Knowledge of the shortest or fastest paths between any two configurations of a particular robot is fundamental. Robots expend resources to achieve tasks. Possibly the simplest resource is time; the minimum amount of time that must be expended to move the robot between configurations is a basic property of the mechanism, and a fundamental metric on the configuration space.

Knowledge of the time optimal trajectories is also useful. Mechanisms should be designed so that common tasks can be achieved efficiently. If the designer must choose between two wheels and three, what is the cost of each choice? Furthermore, the time-optimal metric is independent of compromises made by particular planners or controllers, and therefore provides a useful benchmark to compare them. Finally, the metric derived from the optimal trajectories may be used as a heuristic to guide sampling in complete planning systems that permit obstacles or a more complex dynamic model of the mechanism.

We do not argue that controllers should be designed to drive robots to follow the 'optimal' trajectories we derive, or that planners must use the optimal trajectories as building blocks. Our model ignores the dynamics of real vehicles; this is particularly problematic for larger vehicles. Resources other than time may also be important, including energy consumption, safety, simplicity of programming, sensing opportunities, and accuracy. Trade-offs must be made, but understanding the relative payoffs of each design requires an understanding of the fundamental behavior of the mechanism. The knowledge that great circles are geodesics on the sphere does not require that airplanes must strictly follow great circles, but may nonetheless influence the choice of flight paths.

1.1 Related work

Most of the work on time-optimal control for vehicles has focused on bounded-velocity models of steered cars. Dubins [6] determined the shortest paths between two configurations of a car that can only move forwards at constant speed, with bounded steering angle. Reeds and Shepp [9] found the shortest paths for a steered car that can move backwards as well as forwards. Sussmann and Tang [16] further refined these results, reducing the number of families of trajectories thought to be optimal by two, and Souères and Boissonnat [13], and Souères and Laumond [14] discovered the mapping from pairs of configurations to optimal trajectories for the Reeds and Shepp car.

Desaulniers [5] showed that in the presence of obstacles, shortest paths may not exist between certain configurations of steered cars. Furthermore, in addition to the straight lines and circular arcs of minimum radius discovered by Dubins, the shortest paths may also contain segments that follow the boundaries of obstacles. Vendittelli *et al.* [17] used geometric techniques to develop an algorithm to obtain the shortest non-holonomic distance from

a robot to any point on an obstacle.

Recently, the optimal trajectories have been found for vehicles that are not steered cars, and metrics other than time. The time-optimal controls for differential-drives with independent bounds on the wheel speeds were discovered by Balkcom and Mason [1]. Chitsaz *et al.* [2] determined the trajectories for a differential-drive that minimize the sum of the rotation of the two wheels. The optimal paths have also been explored for some examples of vehicles without wheels. Coombs and Lewis [4] consider a simplified model of a hovercraft, and Chyba and Haberkorn [3] consider underwater vehicles. We know of no previous attempts to obtain closed-form solution for the optimal trajectories for any omni-directional vehicle.

The model of the three-wheeled omni-directional vehicle that we study is similar to that used by Williams *et al.* [12], who are concerned with obtaining a feasible model of friction and wheel-slip, rather than optimal control.

Bounded-velocity models capture the kinematics of a vehicle, but not the dynamics. Our approach specifically allows unbounded accelerations. The durations of optimal trajectories we compute are a lower bound for the durations of optimal trajectories for a more complex dynamic model. Since the unbounded accelerations for our model only occur a small bounded number of times during an optimal trajectory, the trajectories can be time-scaled to yield trajectories that are feasible for systems with significant dynamics, giving both an upper and a lower bound on the duration of the optimal dynamic trajectories. For small robots following sufficiently long trajectories (several robot-lengths in distance), we expect the approximation to be reasonable.

Although the bounded-velocity model is not completely satisfying, the optimal-control problem for dynamic models of ground vehicles appears to be very difficult; the differential equations describing the trajectories do not have recognizable analytical solutions, and in some cases, the optimal trajectories involve chattering, an infinite number of control switches in a finite time [15]. Papers by Reister and Pin [10], and Renaud and Fourquet [11] present numerical and partial geometric results for steered cars, and Kalmár-Nagy *et al.* [7] present algorithms for numerically computing optimal trajectories for a bounded-acceleration model of the omnidirectional robot we consider. However, tight bounds on the optimal-

ity of the derived solutions have proven difficult to determine, as has complete characterization of the geometric structure of trajectories.

2   Model, assumptions, notation

Let the state of the robot be $q = (x, y, \theta)$, the location of the center of the robot, and the angle that the line from the center to the first wheel makes with the horizontal, as shown in figure 1(b). Without loss of generality, we assume that the distance from the center of the robot to the wheels is one. We further assume that each of the three wheel-speed controls v_1, v_2, and v_3 is in the interval $[-1, 1]$. We define the control region

$$U = [-1,1] \times [-1,1] \times [-1,1], \qquad (1)$$

and consider the class of *admissible controls* to be the measurable functions $u(t)$ mapping the time interval $[0, T]$ to U: $u(t) = (v_1(t), v_2(t), v_3(t))^T$.

To simplify notation, we define $c_i = \cos \theta_i$, and $s_i = \sin \theta_i$, where $\theta_i = \theta + (i-1)120°$, the angle of the ith wheel measured from the horizontal. Define the matrix S to be the Jacobian that transforms between configuration-space velocities of the vehicle, and velocities of the wheels in the controlled direction:

$$S = \begin{bmatrix} -s_1 & c_1 & 1 \\ -s_2 & c_2 & 1 \\ -s_3 & c_3 & 1 \end{bmatrix} \qquad (2)$$

$$S^{-1} = \frac{2}{3} \begin{bmatrix} -s_1 & -s_2 & -s_3 \\ c_1 & c_2 & c_3 \\ 1/2 & 1/2 & 1/2 \end{bmatrix}. \qquad (3)$$

We define the state trajectory $q(t) = (x(t), y(t), \theta(t))$ for any initial state q_0 and admissible control $u(t)$ using Lebesgue integration, with the standard measure:

$$q(t) = q_0 + \int S^{-1} u. \qquad (4)$$

For any admissible control, the time derivative $\dot{q}$ is defined almost everywhere, and

$$\dot{q} = S^{-1} u = \frac{2}{3} \begin{bmatrix} -s_1 & -s_2 & -s_3 \\ c_1 & c_2 & c_3 \\ 1/2 & 1/2 & 1/2 \end{bmatrix} \begin{pmatrix} v_1 \\ v_2 \\ v_3 \end{pmatrix}. \qquad (5)$$

It may be easily verified that the kinematic equations and bounds on the controls satisfy the conditions of theorem 6 of Sussmann and Tang [16]; an optimal trajectory exists between every pair of start and goal configurations.

3 Pontryagin's Maximum Principle

This section uses Pontryagin's Maximum Principle [8] to derive necessary conditions for time-optimal trajectories. The Maximum Principle states that if the trajectory $q(t)$ with corresponding control $u(t)$ is time-optimal then the following conditions must hold:

1. There exists a non-trivial (not identically zero) *adjoint function*: an absolutely continuous $\mathbf{R}^3$-valued function of time, $\lambda(t)$,

$$\lambda(t) = \begin{pmatrix} \lambda_1(t) \\ \lambda_2(t) \\ \lambda_3(t) \end{pmatrix},$$

   defined by a differential equation, the *adjoint equation*, in the configuration and in time-derivatives of the configuration:

$$\dot{\lambda} = -\frac{\partial}{\partial q}\langle \lambda, \dot{q}(q, u) \rangle \quad \text{a.e.,} \tag{6}$$

   where angle brackets denote the dot product. We call the inner product appearing in equation 6 the *Hamiltonian*:

$$H(\lambda, q, u) = \langle \lambda, \dot{q}(q, u) \rangle. \tag{7}$$

2. The control $u(t)$ minimizes the Hamiltonian:

$$H(\lambda(t), q(t), u(t)) = \min_{z \in U} H(\lambda(t), q(t), z) \quad \text{a.e.} \tag{8}$$

   Equation 8 is called the *minimization equation*.

3. The Hamiltonian is constant and non-positive over the trajectory. We define λ_0 as the negative of the value of the Hamiltonian; λ_0 is constant and non-negative for any optimal trajectory.

3.1 Application of the Maximum Principle

We solve for the adjoint vector by direct integration of equation 6:

$$\lambda_1 = 3k_1 \tag{9}$$
$$\lambda_2 = 3k_2 \tag{10}$$
$$\lambda_3 = 3(k_1 y - k_2 x + k_3), \tag{11}$$

where $3k_1$, $3k_2$, and $3k_3$ are constants of integration. (The constant factor of 3 will simplify the form of equations 14, 15, and 16 below.)

We now substitute the adjoint function into the minimization equation to determine necessary conditions for time-optimal trajectories. To simplify notation, we define three functions,

$$\varphi_i(t) = \langle \lambda(t), f_i(q(t)) \rangle, \tag{12}$$

where f_i is the ith column of S^{-1}. Explicitly, if we define the function

$$\eta(x, y) = k_1 y - k_2 x + k_3, \tag{13}$$

then the functions are:

$$\varphi_1 = 2(-k_1 s_1 + k_2 c_1) + \eta(x, y) \tag{14}$$
$$\varphi_2 = 2(-k_1 s_2 + k_2 c_2) + \eta(x, y) \tag{15}$$
$$\varphi_3 = 2(-k_1 s_2 + k_2 c_2) + \eta(x, y). \tag{16}$$

We may now write the equation for the Hamiltonian in terms of these functions and the controls v_1, v_2, and v_3:

$$H = \varphi_1 v_1 + \varphi_2 v_2 + \varphi_3 v_3. \tag{17}$$

The minimization condition of the Maximum Principle (condition 2, above) applied to equation 17 implies that if the function φ_i is negative, then v_i should be chosen to take its maximum possible value, 1, in order to minimize H. If the function φ_i is positive, then v_i should be chosen to be -1. Since the controls switch whenever one of the functions φ_i changes sign, we refer to the functions φ_i as *switching functions*.

Theorem 1 *For any time-optimal trajectory of the omnidirectional vehicle, there exist constants k_1, k_2, and k_3, with $k_1^2 + k_2^2 + k_3^2 \neq 0$, such that at almost every time t,*

the value of the control v_i is determined by the sign of the switching function φ_i:

$$v_i = \begin{cases} 1 & \text{if } \varphi_i < 0 \\ -1 & \text{if } \varphi_i > 0, \end{cases} \qquad (18)$$

where the switching functions φ_1, φ_2, and φ_3 are given by equations 13, 14, 15, and 16. Furthermore, the quantity λ_0 defined by

$$\lambda_0 = -H(\varphi_1, \varphi_2, \varphi_3) = |\varphi_1| + |\varphi_2| + |\varphi_3| \qquad (19)$$

is constant along the trajectory.

    Proof: Application of the Maximum Principle. ∎

The Maximum Principle does not directly give information about the optimal controls in the case that one or more of the switching functions φ_i is zero. Theorems 7 and 8 in section 4 will specifically address this case. The Maximum Principle also does not give information about the constants of integration, as these depend on the initial and final configurations of the robot. In this paper, we give the structure of trajectories as a function of these constants, but do not describe how to determine the constants except in a few cases.

3.2 Geometric interpretation of the switching functions

The switching functions have a geometric interpretation. Consider the function $\eta(x, y)$:

$$\eta(x, y) = k_1 y - k_2 x + k_3. \qquad (20)$$

$\eta(x, y)$ gives the signed, scaled distance of the point (x, y) from a line in the plane whose location is determined by the constants k_1, k_2, and k_3. (If $k_1^2 + k_2^2 = 0$, we may consider the line to be 'at infinity'.) We will call this line the *switching line*. We also associate a direction with the switching line such that any point (x, y) is to the left of the switching line if $\eta(x, y) > 0$, and to the right of the switching line if $\eta(x, y) < 0$.

Theorem 2 *Define the points S_1, S_2, and S_3 rigidly attached to the vehicle, with distance 2 from the center of the vehicle, and making angles of $180°$, $300°$, and $60°$*
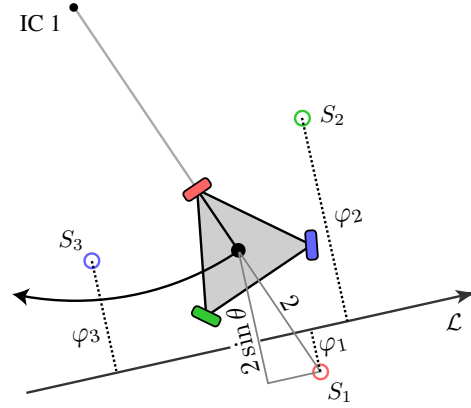
Figure 2: Geometric interpretation of the switching functions. For the case shown, $\varphi_1 < 0$, $\varphi_2 > 0$, and $\varphi_3 > 0$, so the controls are $v_1 = 1$, $v_2 = -1$, and $v_3 = -1$.

with the ray from the center of the vehicle to wheel 1, respectively (refer to figure 2). For any time-optimal trajectory, there exist constants k_1, k_2, and k_3, and a line (the switching line)

$$\mathcal{L} = \{(a, b) \in \mathbf{R}^2 : k_1 b - k_2 a + k_3 = 0\},$$

such that the controls of the vehicle v_1, v_2, and v_3 depend on the location of the points S_1, S_2, and S_3 relative to the line. Specifically, for $i \in \{1, 2, 3\}$,

$$v_i = \begin{cases} 1 & \text{if } S_i \text{ is to the right of the switching line,} \\ -1 & \text{if } S_i \text{ is to the left of the switching line.} \end{cases}$$

    Proof: Let (x_{S_i}, y_{S_i}) be the coordinates of S_i. We compute the signed, scaled distance of the point S_i from the line $\mathcal{L}$, and observe from the definition of the switching functions that $\varphi_i(x, y, \theta) = \eta(x_{S_i}, y_{S_i})$. ∎

We will call S_1, S_2, and S_3 the *switching points*. For any optimal trajectory, the location of the switching line is fixed by the choice of constants, and the controls at any point depend on the signs, but not on the magnitudes, of the switching functions. Figure 2 shows an example. Two of the switching points (S_2 and S_3) are to the left of the switching line, so the corresponding switching functions are positive, and wheels 2 and 3 spin at full speed in the negative direction. The remaining switching point (S_1) is to the right of the switching line, so wheel 1 spins at full speed in the positive direction. As a result of these

controls, the robot will follow a clockwise circular arc. The center of the arc is a distance of four from the robot, and along the line containing the center of the robot and wheel 1.

If all three switching functions have the same sign, the controls all take either their maximum or minimum value, and the robot spins in place. The center of rotation is the center of the robot; we call this point IC 0. If the switching functions are non-zero but do not all have the same sign, the vehicle rotates in a circular arc. The rotation center is a distance of four from the center of the robot, on the ray connecting the center of the robot and the wheel corresponding to the 'minority' switching function. We call the rotation centers corresponding to each wheel IC 1, IC 2, and IC 3.

The switching functions are invariant to translation of the vehicle parallel to the switching line (see figure 2), and scaling the switching functions by a positive constant does not affect the controls. Therefore, for any optimal trajectory, we may without loss of generality choose a coordinate frame with x-axis on the switching line, and an appropriate scaling, such that y gives the distance from the switching line, and θ gives the angle of the vehicle relative to the switching line. With this choice of coordinates, the switching functions become

$$\varphi_1 = y - 2s_1 \qquad (21)$$
$$\varphi_2 = y - 2s_2 \qquad (22)$$
$$\varphi_3 = y - 2s_3 . \qquad (23)$$

We will use these coordinates for the remainder of the paper.

4   Properties of extremals

We will say that any trajectory that satisfies the conditions of theorem 1 (or equivalently, theorem 2) is *extremal*. In this section, we will enumerate several properties of extremal trajectories. The primary result is that every extremal trajectory contains only a finite number of control switches with an upper bound determined by λ_0. The first-time reader may wish to skip the technical details in this section, and return to it after sections 5 and 6, which describe the geometric structure of optimal trajectories.

We say that an extremal trajectory is *generic* on some interval if none of the switching functions φ_i is zero at any

point contained in the interval. We say that a trajectory is *singular* on some interval if exactly one of the switching functions is identically zero on that interval, and no other switching function is zero at any point on the interval. We say that an extremal trajectory is *doubly-singular* on an interval if exactly two of the switching functions are zero on that interval, and the third switching function is never zero on the interval.

Theorem 3 *The negative of the Hamiltonian achieves a global minimum if and only if the trajectory is doubly-singular at that point; at a doubly-singular point, $\lambda_0 = 3$.*

Proof: We can compute an expression for the Hamiltonian using relations between the switching functions. Notice that $s_1 + s_2 + s_3 = 0$, from the trigonometric identities. Adding the three switching functions from equations 21 – 23,

$$\varphi_1 + \varphi_2 + \varphi_3 = 3y . \qquad (24)$$

Also, for distinct $i, j, k \in \{1, 2, 3\}$,

$$\varphi_i + \varphi_j - \varphi_k = y - 2s_i - 2s_j + 2s_k \qquad (25)$$
$$= y - 2(s_i + s_j + s_k) + 4s_k \qquad (26)$$
$$= y + 4s_k . \qquad (27)$$

The equation for the negative of the Hamiltonian in terms of y and θ is therefore

$$-H(y, \theta) = \begin{cases} |3y| & \text{if } \varphi_1, \varphi_2, \varphi_3 \text{ have same sign} \\ |y + 4s_k| & \text{otherwise.} \end{cases} \qquad (28)$$

Level sets of this function are shown in figure 6. We divide the domain into two pieces. First consider the domain $(y, \theta) \in R/[-2, 2] \times S^1$. The minimum value for λ_0 is 6 on this domain, since the switching functions have the same sign. Now consider the domain $(y, \theta) \in [-2, 2] \times S^1$. On this compact domain, H is continuous, and achieves both a minimum and a maximum.

At any minimum point that is not along the boundary, either (i) the partial derivatives of H are both zero, or (ii), the partial derivatives of H are discontinuous. The partial $\delta H/\delta y$ is nonzero everywhere ($= 3$ or $= 1$ depending on the signs of the switching functions). Therefore the partials are discontinuous at the minimum. $\delta H/\delta y$ is discontinuous iff $\varphi_i = 0$ for some $i \in \{1, 2, 3\}$.

Consider a root of the ith switching function. Let φ_j and φ_k be the values of the other switching functions, with k and j chosen such that wheels i, j, and k are in clockwise order. Evaluating equations 19, 21, 22, and 23 at this root,

$$\lambda_0 = |\varphi_j| + |\varphi_k|, \tag{29}$$
$$y = 2\sin\theta_i. \tag{30}$$

From equations 24 and 30,

$$\varphi_j + \varphi_k = 6\sin\theta_i \tag{31}$$
$$\varphi_k - \varphi_j = 2\sqrt{3}\cos\theta_i. \tag{32}$$

We may now write λ_0 in terms of θ and the signs on the switching functions:

$$\lambda_0 = \begin{cases} 6\sin\theta_i & \text{if } \varphi_j \geq 0 \text{ and } \varphi_k \geq 0. \\ -6\sin\theta_i & \text{if } \varphi_j \leq 0 \text{ and } \varphi_k \leq 0. \\ 2\sqrt{3}\cos\theta_i & \text{if } \varphi_j \leq 0 \text{ and } \varphi_k \geq 0. \\ -2\sqrt{3}\cos\theta_i & \text{if } \varphi_j \geq 0 \text{ and } \varphi_k \leq 0. \end{cases} \tag{33}$$

The minimum value of this function is $\lambda_0 = 3$, and the minima occur at $\theta_i \in \{30°, 210°\}$; at these points, $\varphi_j = 0$, so the trajectory is doubly-singular. ∎

Corollary 1 *At no point along an extremal trajectory does $\varphi_1 = \varphi_2 = \varphi_3 = 0$.*

Proof: If $\varphi_1 = \varphi_2 = \varphi_3 = 0$ then $\lambda_0 = 0$. ∎

Corollary 2 *If an extremal trajectory contains any doubly-singular point, then every point of the trajectory is doubly-singular.*

Proof: The Maximum Principle implies that the Hamiltonian must remain constant over any extremal trajectory; the previous theorem tells us that any trajectory that contains both points that are doubly-singular points and points that are not cannot have a constant Hamiltonian. ∎

Theorem 4 *Every pair of singular points of an extremal trajectory is contained in a single singular interval, or is separated by a generic point.*

Proof: Let t_1 and t_4 be two arbitrary times at which the trajectory is singular, with $t_4 > t_1$. Let i and j be the indices of the switching functions that are zero; $\varphi_i(t_1) = \varphi_j(t_4) = 0$. If t_1 and t_4 are not contained within the same singular interval, continuity of the switching functions implies that then there must be a time such that either the switching function that was initially zero becomes non-zero, or some switching function that was initially non-zero becomes zero. That is, there exists a time $t_3 \in [t_1, t_4]$ such that at least one of the following properties hold:

1. $\varphi_i(t_3) \neq 0$,

2. $\varphi_k(t_3) = 0$ for some $k \neq i$ (from continuity of φ_j).

If the first property holds, but not the second, then t_3 is a generic point. If the second property holds, but not the first, t_3 is a doubly-singular point, and the trajectory is not extremal by corollaries 1 and 2. If both properties hold, then by the intermediate value theorem, there must be a point $t_2 \in [t_1, t_3]$ such that either $\varphi_i(t_2) = \varphi_k(t_2)$, or $\varphi_i(t_2) = -\varphi_k(t_2)$. This point must be generic, since it cannot be doubly-singular. ∎

Lemma 1 *Assume t_1 and t_2 are two points of a generic interval, with $t_2 > t_1$. Define δ to be the duration of the interval $[t_1, t_2]$. If $\theta(t_1) \neq \theta(t_2)$, then*

$$\delta \geq |\theta(t_2) - \theta(t_1)| \tag{34}$$

If $\theta(t_1) = \theta(t_2)$, then

$$\delta \geq 2\pi. \tag{35}$$

Proof: On any generic interval, the controls are constant and $\dot\theta$ is a non-zero constant. Depending on the signs of the switching functions, $\dot\theta = \pm 1$, or $\dot\theta = \pm 1/3$. The properties follow immediately from direct integration of $\dot\theta$. ∎

Theorem 5 *Every generic point is contained in a generic interval that either has the start or the end of the entire trajectory as an endpoint, or has a duration that is lower-bounded by a constant, δ, that depends only on λ_0.*

Proof: Continuity of the switching functions implies that every generic point is contained in an open interval containing only generic points. Consider the largest

open interval that contains the generic point; the interval is bounded either by singular points, or by the start and end of the trajectory. We will show that singular points are separated by a constant δ that depends only on λ_0.

Given a value for λ_0, there exist a finite number of real-valued solutions for θ, which may all be found by solving the above equations for θ.

Assume now that the generic interval is bounded by two singular points, t_1 and t_2, with $t_2 > t_1$. We may compute all possible values for $\theta(t_1)$ and $\theta(t_2)$ in terms of λ_0. Consider all possible pairs of $\theta(t_1)$ and $\theta(t_2)$, and the angular distance between $\theta(t_2)$ and $\theta(t_1)$ for each pair. If all distances are zero, then let $\delta = 2\pi$; otherwise, let δ be the minimum non-zero distance. The duration of the interval must be at least δ, by lemma 1. ∎

Theorem 6 *The number of control switches in an extremal trajectory is finite, and upper-bounded by a constant that depends only on λ_0.*

Proof: Let N be the number of switches. By corollary 2, the trajectory is doubly-singular everywhere, or nowhere. If the trajectory is doubly-singular, then $N = 0$. Otherwise, let T be the duration of the trajectory. Since every maximal generic interval (except possibly the first and the last) is contained in an interval of duration of at least δ (theorem 5), there can be no more than $T/\delta + 2$ maximal generic intervals, and

$$N \leq \frac{T}{\delta} + 2. \tag{36}$$

∎

In section 7, we will show that for *optimal* trajectories, a much stronger property holds: the number of control switches is never greater than 18.

Theorem 7 *Consider a singular interval of non-zero duration, with $\varphi_i = 0$. At every point of the interval, $y = \sin\theta_i = 0$, and the controls are constant: $v_i = 0$, and $v_j = -v_k = \pm 1$.*

Proof: Choose an arbitrary point on the interior of the interval. First, assume that φ_j and φ_k have the same sign. Then $v_j = v_k = \pm 1$, by theorem 1. From the system equations (5),

$$\dot{\theta} = \frac{1}{3}(v_i \pm 2) \neq 0. \tag{37}$$

From equation 33, the time derivative of λ_0 is

$$\dot{\lambda}_0 = \pm 6\dot{\theta}\cos\theta_i = 0. \tag{38}$$

The fact that $\dot{\theta} \neq 0$ implies that $\cos\theta_i = 0$ can hold only instantaneously, and therefore the interval must be of zero duration.

Symbol	φ	u	λ_0
P_-	+++	-1, -1, -1	$3y$
P_+	---	1, 1, 1	$-3y$
C_{1-}	-++	1, -1, -1	$y + 4\sin\theta_1$
C_{2-}	+-+	-1, 1, -1	$y + 4\sin\theta_2$
C_{3-}	++-	-1, -1, 1	$y + 4\sin\theta_3$
C_{1+}	+--	-1, 1, 1	$-y - 4\sin\theta_1$
C_{2+}	-+-	1, -1, 1	$-y - 4\sin\theta_2$
C_{3+}	--+	1, 1, -1	$-y - 4\sin\theta_3$
$S_{1,3}$	-0+	1, 0, -1	$2\sqrt{3}$
$S_{1,2}$	-+0	1, -1, 0	$2\sqrt{3}$
$S_{3,2}$	0+-	0, -1, 1	$2\sqrt{3}$
$S_{3,1}$	+0-	-1, 0, 1	$2\sqrt{3}$
$S_{2,1}$	+-0	-1, 1, 0	$2\sqrt{3}$
$S_{2,3}$	0-+	0, 1, -1	$2\sqrt{3}$
D_{3+}	00+	.5, .5, -1	3
D_{1-}	-00	1, -.5, -.5	3
D_{2+}	0+0	.5, -1, .5	3
D_{3-}	00-	-.5, -.5, 1	3
D_{1+}	+00	-1, .5, .5	3
D_{2-}	0-0	-.5, 1, -.5	3

Table 1: The twenty extremal controls.

Now assume that φ_j and φ_k have opposite signs. $v_j = -v_k = \pm 1$, by theorem 1. We will first show that

$$y = \sin\theta_i = 0. \tag{39}$$

Assume the converse. If either $y \neq 0$ or $\sin\theta_i \neq 0$, then neither $y = 0$ nor $\sin\theta_i = 0$, since $y = 2\sin\theta_i$. From equation 33, we can write the time derivative of λ_0:

$$\dot{\lambda}_0 = \pm 2\sqrt{3}\dot{\theta}\sin\theta_i \tag{40}$$

Since λ_0 must be constant over an extremal trajectory, it follows that $\dot{\theta} = 0$. From equations 21, 22, and 23,

$$\dot{y} = 2\dot{\theta}\cos\theta_i = 0. \tag{41}$$

From the system equations (5),

$$\dot{\theta} = \frac{1}{3}(v_i + v_j + v_k) = 0 \qquad (42)$$

$$\dot{y} = \frac{2}{3}(c_i v_i + c_j v_j + c_k v_k) = 0. \qquad (43)$$

Combining these equations, and using the fact that $v_j = -v_k$, we can show that $c_j = c_k$, which implies that $\sin\theta_i = 0$, a contradiction. Therefore, $y = s_i = 0$ over the entire interval. From the system equations, it follows that $v_i = 0$. ∎

Theorem 8 *Consider a doubly-singular interval of non-zero duration, with $\varphi_i = \varphi_j = 0$. Along the interval, (i) $y = \pm 1$, $\cos\theta_k = 0$, and (ii) the controls are constant, with $v_k = \pm 1$, and $v_i = v_j = \mp.5$.*

Proof: Property (i) follows from equations 21, 22, and 23. Property (ii) can then be shown by taking a time derivative of the equations given in property (i) and applying the system equations (5). ∎

5 Extremal controls

Theorems 1, 6, 7, and 8 imply that optimal trajectories are composed of a finite number of segments, along each of which the controls are constant. Considering all possible combinations of signs and zeros of the switching functions allows the twenty extremal controls to be enumerated; table 1 shows the results. The vehicle may spin in place, follow a circular arc, translate in a direction perpendicular to the line joining two wheels, or translate in a direction parallel to the line joining two wheels. We denote each control by a symbol: $P_\pm$, $C_{i\pm}$, $S_{i,j}$, or $D_{k\pm}$, respectively. The subscripts depend on the specific signs of the switching functions.

Theorem 2 gives a more geometric interpretation of the extremal controls. The controls depend on the location of the switching points relative to the switching line. There are four cases:

- **Spin in place.** If the vehicle is far from the switching line, all of the switching points are on the same side of the line, and all of the wheels spin in the same direction. Figure 3(a) shows an example. If the robot is
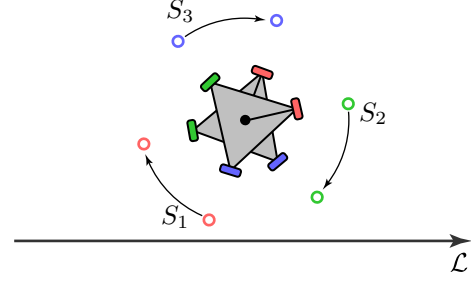
(a) An example clockwise *spin* control, P_-.
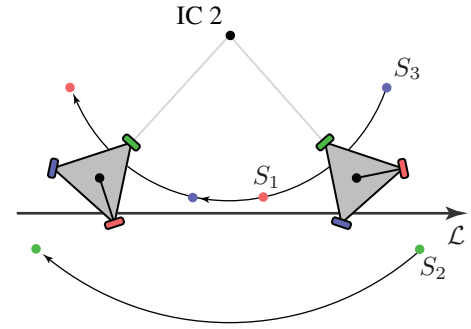
(b) An example clockwise *circular arc* control, C_{2-}.
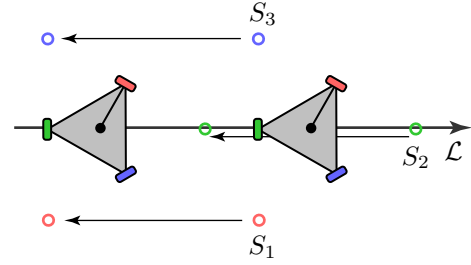
(c) An example *singular translation* control, $S_{1,3}$.
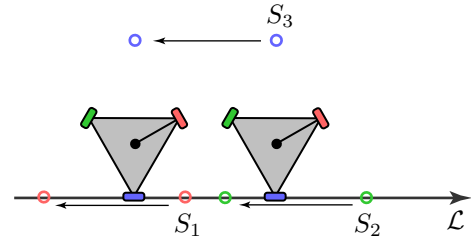
(d) An example *doubly-singular translation* control, D_{3+}.

Figure 3: Extremal controls for an omni-directional robot.

to the left of the switching line, the robot spins clockwise (P_-); if the robot is to the right of the switching line, the robot spins counterclockwise (P_+).

- **Circular arc.** Figure 3(b) shows an example of a counterclockwise arc around IC 2 (C_{2+}). If two switching points are on one side of the line, and one switching point is on the other side, two wheels spin in one direction at full speed, and one wheel spins in the opposite direction at full speed. These controls cause the vehicle to follow a circular arc of radius four; the center of the arc is the IC corresponding to the switching point that is not on the same side of the switching line as the others, and the direction of rotation depends on whether this switching point is to the left or right of the line.

- **Singular translation.** Figure 3(c) shows an example, $S_{1,3}$, where the second switching point slides along the switching line. If two switching points are an equal distance from the switching line but on opposite sides of the line, two of the wheels spin at full speed, but in opposite direction. If the last switching point falls exactly on the switching line, theorem 2 does not provide any information about the speed of the last wheel. If the wheel does not spin, then the vehicle translates along the switching line, as described by theorem 7. Otherwise, the singular translation is only instantaneous.

- **Doubly-singular translation.** Figure 3(b) shows an example, D_{3+}, where the first and second switching points slide along the switching line. If two switching points fall on the switching line, the speeds of the corresponding wheels cannot be determined from theorem 2. If these wheels spin at half speed, in a direction opposite to that of the third wheel, both switching points slide along the switching line, and the vehicle translates. It turns out that that doubly-singular controls, although extremal, are *never* optimal; see section 7.

(a) A **RollCW** trajectory, $C_{2-}P_-C_{3-}P_-C_{1-}$.

(b) A **Shuffle** trajectory, $C_{3+}C_{1-}P_-C_{2-}C_{3+}C_{1-}P_-\ldots$

(c) A **Tangent** trajectory, $C_{2-}^{\mathrm{start}}S_{2,3}C_{2-}^{\mathrm{mid}}S_{2,1}C_{2-}^{\mathrm{end}}P_-C_{3-}^{\mathrm{start}}$.
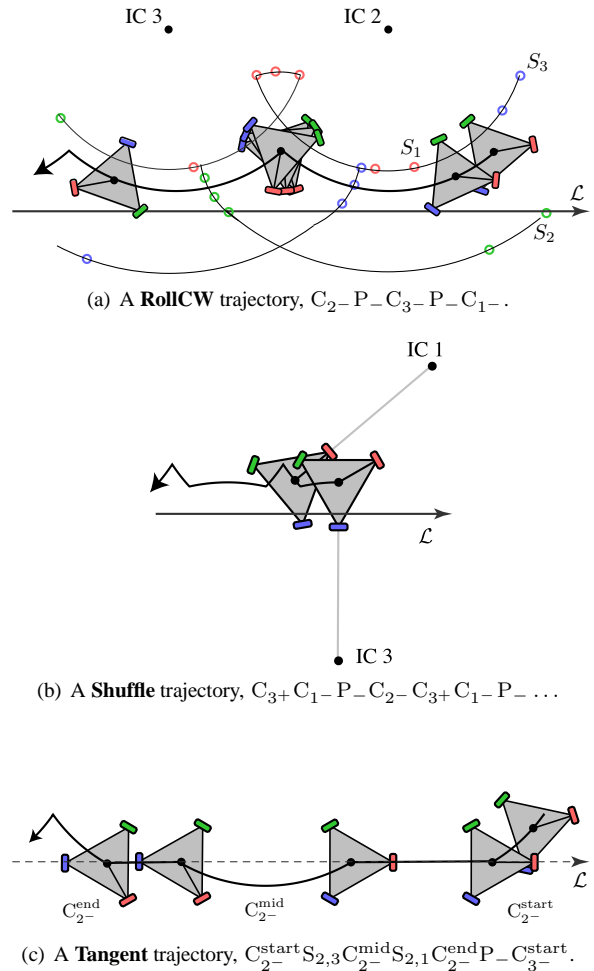
Figure 4: Extremal trajectories for an omni-directional robot.

10

6 Classification of extremal trajectories

Every extremal trajectory is generated by a sequence of constant controls from table 1. However, not every sequence is extremal. This section geometrically enumerates the five structures of extremal trajectories.

First consider an example, shown in figure 4(a). Initially, switching points 1 and 3 fall to the left of the switching line, and switching point 2 falls to the right of the switching line. The vehicle rotates in the clockwise direction about IC 2. After some amount of rotation, switching point 2 crosses the switching line. Now all three switching points are to the left of the switching line, the velocity of wheel 2 changes sign, and the vehicle spins in place. When switching point 3 crosses the switching line, the vehicle begins to rotate about IC 3. When switching point 3 crosses back to the left side, the vehicle spins in place again until switching point 1 crosses the line. The pattern continues in this form; we describe the trajectory by the sequence of symbols $C_{2-} P_{-} C_{3-} P_{-} C_{1-}$.

In general, if no switching points fall on the switching line (the generic case), then the controls are completely determined by theorem 2, and the vehicle either spins in place or rotates around a fixed point. When one of the switching points crosses the switching line, the controls change. For some configurations for which one or two of the switching points fall exactly on the switching line (the singular and doubly-singular cases), there exist controls that allow the switching points to slide along the switching line.

We will define these classes more rigorously in sections 6.1 and 6.2. However, we can see geometrically that there are five cases:

- **SpinCW** and **SpinCCW**. If the vehicle is far from the switching line, the switching points are on the same side of the switching line and never cross it; the vehicle spins in place indefinitely. The structure off the trajectory is either P_{-} (if the vehicle is to the left of the switching line) or P_{+} (if the vehicle is to the right of the switching line). An example is shown in figure 3(a).

- **RollCW** and **RollCCW**. If the switching points either straddle the switching line, or the vehicle is close enough to the switching line that spinning in place will eventually cause the switching points to straddle the line, the trajectory is a sequence of circular arcs and spins in place. If the vehicle is far enough from the switching line that every switching point crosses the switching line and returns to the same side before the next switching point crosses the line, the structure of the trajectory is as described in the example above and in figure 4(a).

- **Shuffle**. If the vehicle is close enough to the switching line that two switching points cross the switching line before the first returns to its initial side, the sign of $\dot{\theta}$ changes during the trajectory. An example is shown in figure 4(b).

- **Tangent**. As the vehicle spins in place or follows a circular arc, the switching points follow circular arcs. If one of these arcs is tangent to the switching line, a singular control becomes possible at the point of tangency, and the vehicle may translate along the switching line for an arbitrary duration before returning to following a circular arc. An example is shown in figure 4(c). A single circular arc is divided into three sections in a *tangent* trajectory. These segments are separated by the singular S straights, possibly of zero duration. We call the arc sections C^{start}, C^{mid}, and C^{end}, as shown in figure 4(c). The robot rotates through $60°$ during a complete C^{mid} segment.

- **Slide**. If two switching points fall on the switching line, the trajectory is doubly singular. The vehicle slides along the switching line in a pure translation; an example of this trajectory type is shown by figure 3(d). Although *slide* trajectories are extremal, we will show in section 7 that they are never optimal.

6.1 Configuration space

In order to show that the above list of trajectory classes is exhaustive, it is useful to consider the structure of trajectories in configuration space. The configuration of the robot relative to the switching line may be represented by (θ, y). Figure 6(a) shows the configuration space.

Each point on figure 6(a) corresponds to a configuration of the robot relative to the switching line. The

Class	Control sequence	Value of λ_0
SpinCW	P_-	$\lambda_0 \geq 6$
SpinCCW	P_+	
RollCW	$C_{3-}P_-C_{2-}P_-C_{1-}P_- \ldots$	$2\sqrt{3} \leq \lambda_0 < 6$
RollCCW	$C_{1+}P_+C_{2+}P_+C_{3+}P_+ \ldots$	
Tangent	$CSCSCP \ldots$	$\lambda_0 = 2\sqrt{3}$
Shuffle_{1-}	$C_{2+}C_{1-}C_{3+}P_+ \ldots$	$3 < \lambda_0 < 2\sqrt{3}$
Shuffle_{2-}	$C_{3+}C_{2-}C_{1+}P_+ \ldots$	
Shuffle_{3-}	$C_{1+}C_{3-}C_{2+}P_+ \ldots$	
Shuffle_{1+}	$C_{3-}C_{1+}C_{2-}P_- \ldots$	
Shuffle_{2+}	$C_{1-}C_{2+}C_{3-}P_- \ldots$	
Shuffle_{3+}	$C_{2-}C_{3+}C_{1-}P_- \ldots$	

Table 2: Four of the five classes of extremal trajectories. Every optimal trajectory is composed of a sequence of controls that is a subsequence of one of the above types. (Doubly-singular *slide* trajectories are extremal, but never optimal; see section 7.) The structure of *tangent* trajectories is complicated, and shown explicitly in figure 5.
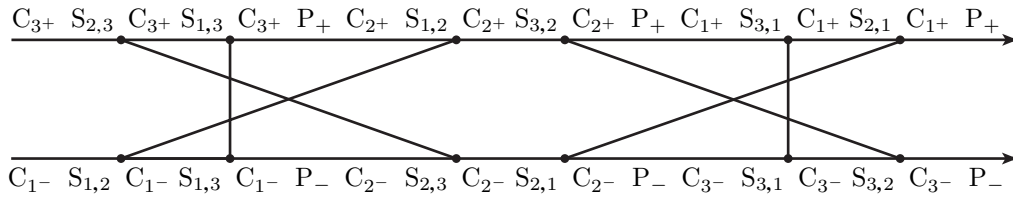
Figure 5: The structure of *tangent* trajectories. The controls must occur in left-to-right order in the direction shown by either the top or the bottom arrows. However, after a singular control S, the trajectory may switch from one sequence to the other, as shown by the vertical and diagonal lines segments.

sinusoidal curves defined by $\varphi_1 = 0$, $\varphi_2 = 0$, and $\varphi_3 = 0$ mark boundaries in configuration space; we call these curves the *switching curves*. The switching curves and their intersections divide the configuration space into cells, within each of which the controls are constant.

As an example, consider any point below switching curve 1, but above switching curves 2 and 3. The controls are $(-1, 1, 1)$, described by the symbol C_{1-}; the vehicle follows a circular arc around IC 1 in the clockwise direction. This trajectory is a sinusoidal curve in configuration space.

6.2 Level sets of the Hamiltonian

The trajectory curves in configuration space can be drawn by considering each possible initial configuration, determining the constant control, and integrating to find the tra-

jectory. When the trajectory crosses a switching curve, the control switches. However, the condition that the Hamiltonian remain constant over a trajectory provides an even simpler way to enumerate all trajectories in the configuration space.

Over any particular trajectory, $H = -\lambda_0$, for some constant $\lambda_0 \in R^+$. Different values of λ_0 correspond to different types of trajectories. For example, assume $\lambda_0 = 9$. All three switching functions must be positive, and equation 28 reduces to $y = \pm 3$. Thus, $\lambda_0 = 9$ corresponds to trajectories for which y is constant, and only θ changes; *i.e.*, a 'spin' trajectory. For any $\lambda_0 \geq 6$, a similar reasoning hold; the trajectory is a spin.

Figure 6(b) shows the level sets of the Hamiltonian, or equivalently, extremal trajectories in configuration space. The cases are:
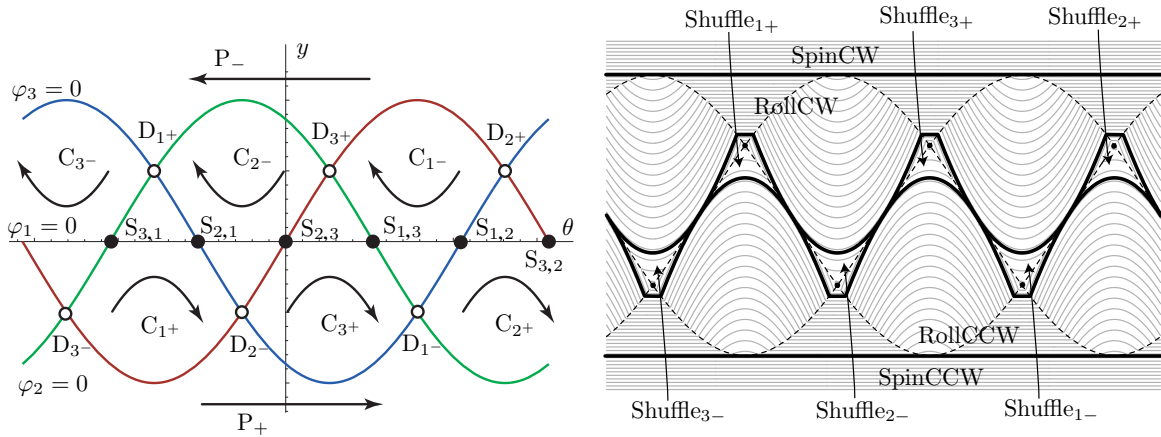
(a) The sinusoidal switching curves partition the configuration space into eight C and P control regions.

(b) The configuration space of the robot relative to the switching line, with level sets of the Hamiltonian. (Axes, not drawn, are the same as for figure 6(a).) Since the Hamiltonian is constant over any optimal trajectory, optimal trajectories lie along contours of the Hamiltonian. The dashed lines represent control switches as shown in figure 6(a); the bold lines separate the trajectory classes.

Figure 6: The configuration space of the robot relative to the switching line.

- If $\lambda_0 > 6$, the level set is a pair of horizontal lines, one with $y = \lambda_0/3$, corresponding to a *spinCW* trajectory, and one with $y = -\lambda_0/3$, corresponding to a *spinCCW* trajectory.

- If $2\sqrt{3} \leq \lambda_0 \leq 6$, the level set is composed of two disjoint curves, one corresponding to a *rollCW* trajectory and one corresponding to a *rollCCW* trajectory.

- If $\lambda_0 = 2\sqrt{3}$, the level set is the union of the bold curves shown in figure 6(b). *Tangent* trajectories follow these curves.

- If $3 < \lambda_0 < 2\sqrt{3}$, the level set is composed of six disjoint curves, one corresponding to each of the six symmetric *shuffle* trajectories.

- If $\lambda_0 = 3$, the level set is six isolated points, each corresponding to one of the six *slide* trajectories.
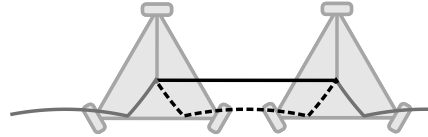
Figure 7: Any sufficiently-short *slide* trajectory (solid line) can be replaced by a faster *shuffle* trajectory (dashed line).

7 Optimal trajectories

We have presented the five classes of extremal trajectory; every optimal trajectory must be extremal. However, not all extremal trajectories are optimal. In this section, we will derive further conditions that optimal trajectories must satisfy. Specifically, we will show that doubly-singular *slide* trajectories are never optimal, and that the number of control switches in any optimal trajectory never exceeds 18. Finally, we show that the classification {*spin*, *roll*, *shuffle*, *tangent*} is *minimal*; for each trajectory class, there exists at least one pair of configurations for which a trajectory of that class is optimal.

Theorem 9 *Doubly-singular slide trajectories are not*

optimal for any pair of start and goal configurations.

Proof: It can be shown (by continuity of equation 44, below) that there is a PCCCP one-period *shuffle* that connects any two configurations on a slide that are separated by less than $8\sqrt{6}/3$; see figure 7. Let t be the duration of the *shuffle*, and let x be the signed distance traveled along the switching line. During any generic interval, the robot moves in a circle or spins in place. We can therefore therefore explicitly write the x and y distances travelled during a single period of a shuffle as a function of the angular distance θ through which the robot turns. If we use equation 33 to eliminate θ in favor of λ_0, we get an equation for the net translation of a single period of a shuffle in terms of λ_0, the characteristic constant for the trajectory:

$$x(\lambda_0) = \frac{-4}{3}\sqrt{36 - \lambda_0^2} + 4\sqrt{12 - \lambda_0^2} \qquad (44)$$

$$t(\lambda_0) = \frac{8\pi}{3} - 12 \arccos \frac{\lambda_0}{2\sqrt{3}} - 4 \arcsin \frac{\lambda_0}{6}. \qquad (45)$$

The forward velocity of a doubly-singular trajectory is -1. We will show that the average forward velocity of the *shuffle* over the length of one period is less than -1 for λ_0 in the interval $(3, 2\sqrt{3})$; *i.e.*, the shuffle is faster. Define

$$v_{\mathrm{avg}}(\lambda_0) = \frac{x(\lambda_0)}{t(\lambda_0)}. \qquad (46)$$

As $\lambda_0 \to 3$,

$$\lim_{\lambda_0 \to 3} v_{\mathrm{avg}} = -1. \qquad (47)$$

We will now show that v_{avg} is monotonically decreasing as λ_0 increases from 3 to $2\sqrt{3}$, by showing that the derivative w.r.t. λ_0 is negative. We will denote differentiation with respect to λ_0 using the prime ($'$) symbol.

$$v'_{\mathrm{avg}} = \frac{tx' - xt'}{t^2} \qquad (48)$$

The term t^2 is strictly positive on the interval, and may be ignored. The numerator is of the form $f(\lambda_0)g(\lambda_0)$, where

$$f(\lambda_0) = \sqrt{12 - \lambda_0^2} - 3\sqrt{36 - \lambda_0^2} \qquad (49)$$

$$g(\lambda_0) = 2\pi\lambda_0 + 9\sqrt{12 - \lambda_0^2} - 3\sqrt{36 - \lambda_0^2} \qquad (50)$$

$$- 9\lambda_0 \arccos \frac{\lambda_0}{2\sqrt{3}} - 3\lambda_0 \arcsin \frac{\lambda_0}{6}.$$

$f(\lambda_0)$ is negative on the interval, so it remains only to show that $g(\lambda_0) > 0$ on the interval. Notice that $g(3) = 0$, so it is sufficient to show that $g'(\lambda_0) > 0$ on the interval. We compute $g'(3) = 0$, and the second derivative of g:

$$g''(\lambda_0) = \frac{9}{\sqrt{12 - \lambda_0^2}} - \frac{3}{\sqrt{36 - \lambda_0^2}}, \qquad (51)$$

which is strictly positive on the interval. ∎

Theorem 10 *Optimal trajectories contain no more than 18 control switches. Specifically,*

(i) *optimal spin trajectories contain zero control switches, and the maximum duration of an optimal spin trajectory is π;*

(ii) *optimal roll trajectories contain at most 8 control switches;*

(iii) *optimal shuffle trajectories contain at most 7 control switches;*

(iv) *optimal tangent trajectories contain at most 12 control switches if the trajectory is non-monotonic in θ, and at most 18 control switches if the trajectory is monotonic in θ;*

The proof for *spin* trajectories is obvious. We consider each of the other trajectory classes separately:

(i) **Roll trajectories:** Consider a *roll* trajectory with 9 or more segments. The trajectory contains a full period beginning with an untruncated spin and ending with an untruncated spin, $\mathrm{PCPCPCP}$. (The additional two segments are required so that even if the trajectory begins or ends on with a truncated spin, a full period is still contained as a subsection.)

There are two cases.

If the circular arcs are at least $60°$, then we cut a $60°$ segment from the center of each arc. We reflect each segment across the switching-line, and adjoin the segments to the original trajectory as shown by the dashed curves in figure 8. After following the first reflected arc, the vehicle is in the same location as if it had followed the original trajectory, but rotated $120°$. After following all three reflected arcs, the

14

vehicle is in the same configuration as if it had followed the original trajectory. Since this equal-cost trajectory is not extremal, neither it nor the original is optimal.

If the rotation segments are less than $60°$, a new non-extremal trajectory of equal or less time may be constructed by reversing the direction of each spin.

(ii) **Shuffle trajectories:** If there are nine switches, then the trajectory must contain the sequence $CPCCCPC$; specifically, it must contain two spins of full duration, as shown in figure 9. Call the first and the last arc in this period A and D; cut the central arc into two symmetric equal-time segments, labeled B and C in the figure. Reordering these segments as C, D, A, B gives an equal-time trajectory. The new trajectory is not extremal, so neither it nor the original is optimal.

(iii) **Tangent trajectories:** The three parts of the C curves appear cyclically in a *tangent* trajectory in the same order, i.e, start, mid, and end (interspersed by the S and the P curves), with possibly different ICs, *e.g.*,

$$C_{3+}^{start}S_{2,3}C_{3+}^{mid}S_{1,3}C_{1-}^{end}P_-C_{2-}^{start}.$$

We divide the *tangent* trajectories into two types:

(a) Trajectories that are **non-monotonic** in θ. We will show that two particular classes of 13-segment non-monotonic *tangent* trajectories are not optimal, by constructing equal-duration trajectories that are not extremal. We then reduce all other non-monotonic cases to these cases.

(b) Trajectories that are **monotonic** in θ. We will show that for any monotonic *tangent* trajectory containing 19 control switches, an equal-duration trajectory containing a 13-segment non-monotonic *tangent* trajectory can be constructed.

If a *tangent* trajectory contains 13 control switches, then it must contain the sequence $CPCSCSCPC$;

Figure 8: The dashed curve show $60°$ arcs reflected from the center of the C segments. After three periods the alternate trajectory leads to the same configuration as the original one.
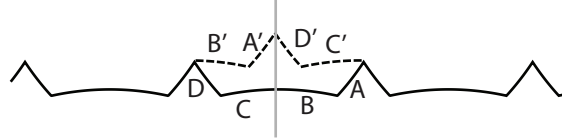
Figure 9: Reordering the segments, as shown by the dashed segments, gives an alternate non-optimal trajectory of the same duration as the original *shuffle* trajectory.

specifically, it must contain two spins P of maximum duration. Two special cases are shown in figure 10. We slice the central C segment and reorder the segments as shown, yielding an equal-time $PCSCPCSCP$ trajectory. Since the constructed trajectory is not extremal, the original trajectory is not optimal.

For the other non-monotonic trajectories the two spins (and the adjoining C^{start} and C^{end} segments) must occur on opposite sides of the switching line. Reflecting the C^{mid} segment and the three segments(C^{start}, C^{end}, and P) that occur on the same side of the switching-line as the C^{mid} segment, as shown in figure 11, gives a trajectory of equal duration as that of one of the two special cases shown in 10.

Now consider monotonic *tangent* trajectories. If the trajectory has 19 switches, then it must contain the sequence $SCSCPCSCSCPCSCS$; *i.e.*, it must contain three full-length C^{mid} central arcs, as shown in figure 12. We can construct an equal-length trajectory containing a non-monotonic *tangent* trajectory with structure $CPCSCSCPC$ by reflecting the C^{mid} segments along the switching-line (see figure 12). This trajectory cannot be optimal, by the argument made above.

∎
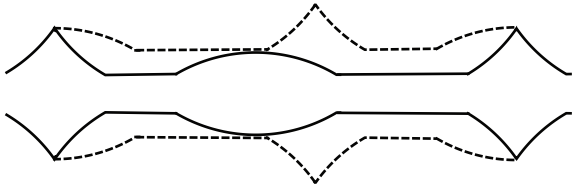
Figure 10: Non-monotonic tangent trajectories that are not optimal. The solid curves represent the actual tangent trajectories. The dashed curves represent alternative trajectories of equal duration that are not extremal.
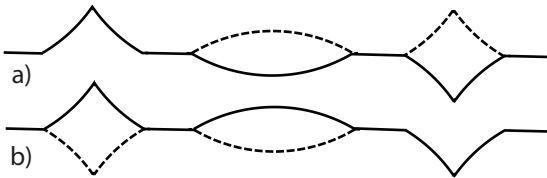
Figure 11: Reducing non-monotonic tangent trajectories to the trajectories shown in figure 10. The solid curves represent the original trajectories. The dashed curves are obtained by reflecting the solid curves across the switching line. The new trajectory obtained is identical to that from figure 10.

Figure 12: Figure for the proof that monotonic trajectories with more than 18 switches are not optimal. The dashed curves are the reflected C^{mid} curves. An equal-time non-monotonic trajectory is created by following the dashed curves instead of the original C^{mid} curves.

Theorem 10 shows that the number of segments for an optimal path between any start and goal are no more than 18. Additionally, for each segment of *roll*, *shuffle*, and *spin* trajectories, we can compute the maximum distance along one of the coordinate axis (x, y, or θ) that the robot can travel. In the next theorem we utilize this knowledge, coupled with the fact that the number of segments is bounded above, to calculate the maximum distance (along one or more coordinate axis) for which these trajectories can be optimal.

Theorem 11 *There exist bounds on the displacements along the x and θ axis beyond which spin, roll, and shuffle trajectories are not optimal. In particular,*

(i) *Roll trajectories with x-displacement more than $\frac{40\sqrt{2}}{\sqrt{3}}$ are not optimal.*

(ii) *Shuffle trajectories with x-displacement more than $\frac{16\sqrt{2}}{\sqrt{3}}$ and θ displacement more than $60°$ are not optimal.*

(iii) *Tangent trajectories are not optimal for configurations that are separated by more than $120°$, with distance between the configurations less than 4.*

Proof: We prove the bounds for each class of trajectory separately.

(i) **Roll trajectories:** Theorem 10 states that *roll* trajectories with more than five C segments are not optimal. Furthermore, the displacement along the x-axis for each complete C segment is the same, and the y displacement for such a segment is zero. The maximum displacement along one such segment is $\frac{8\sqrt{2}}{\sqrt{3}}$.

(ii) **Shuffle trajectories:** *shuffle* trajectories correspond to small parallel-park motions parallel to the x-axis. Like the *roll* trajectories, the limiting case for the maximum distance covered along one period for *shuffle* trajectories occurs as they approach the *tangent* trajectories (see figure 6(b)). The x displacement along this limiting curve is $\frac{8\sqrt{2}}{\sqrt{3}}$. Theorem 10 shows that more than two periods of a *shuffle* trajectory are not optimal.

(iii) **Tangent trajectories:** If the start and goal are separated by more than $120°$, then any *tangent* trajectory connecting the two would need to contain at least one complete $60°$ arc of a circle of radius four. Since all extremal trajectories are monotonic in x, no such *tangent* trajectory can connect start and goal configurations that are closer together than 4.

∎

Theorem 12 *Spin, Roll, Shuffle, and Tangent trajectories are each optimal for at least one pair of start and goal configurations of the omni-directional vehicle.*

Proof: For each class, we explicitly construct a pair of start and goal configurations for which no other trajectory class is optimal.

(i) **Spin.** The maximum value for $|\dot{\theta}|$ along any trajectory is 1. Since spin trajectories achieve this value, a spin trajectory is optimal for any pair of start and goal configurations with the same x and y location.

(ii) **Roll.** Choose any pair of configurations that are separated by more than $120°$, are not at the same (x, y) location, and are closer together than 4.

(iii) **Shuffle.** Consider any one-period shuffle starting and ending in the middle of a spin, and configurations corresponding to the start and finish of this trajectory. The fastest roll between these configurations takes time 2π, since roll trajectories are monotonic in θ; as this is slower than the shuffle, no roll can be optimal. The same is true for monotonic tangent trajectories. Non-monotonic tangent trajectories are a limiting case of tangent trajectories; the duration of a non-monotonic tangent between the two configurations can be lower-bounded by $t(2\sqrt{3})$, which is greater than $t(\lambda_0)$ for any $\lambda_0 < \sqrt{3}$. (See equation 45.)

(iv) **Tangent.** Choose start and goal configurations that are farther apart than the maximum distance of a roll, and that have different start and goal angles. By theorem 11, only tangent trajectories can be optimal.

∎

8 Open problems

We have presented a complete and minimal classification of optimal trajectories, and explicit descriptions of each trajectory. However, we have not addressed the problem of determining which of these trajectories is optimal for a particular pair of start and finish configurations. For the problem of determining the shortest trajectories for a steered car, Reeds and Shepp [9] suggest the simple approach of enumerating all possible structures that connect two configurations, and comparing the time of each. A similar approach should be possible for the omnidirectional vehicle.

Souères and Laumond [14] determined the complete *synthesis* of optimal trajectories for the steered car: an explicit mapping from pairs of configurations to trajectories. Balkcom and Mason [1] determined the synthesis for differential-drive vehicles. Such a result for the omnidirectional vehicle would remove the need for enumerating and comparing all trajectories between a pair of configurations, and would give the metric on the configuration space more explicitly.

The current work also does not consider the presence of obstacles. We expect that optimal trajectories among obstacles would consist of segments of obstacle-free trajectories, and segments that follow the boundary of the obstacles.

There are also broader questions. The shortest or fastest trajectories are now known for a few examples of specific systems: steered cars, the differential drive, and the omnidirectional vehicle considered here. The results share some features in common; each of the optimal trajectories can be described by motion of the robot relative to a switching line in the plane. The trajectories for steered cars include arcs of circles and straight lines; the trajectories for differential drives include spins in place and straight lines. The trajectories for the current system include straight lines, arcs of circles, and spins in place, and the system could in that sense be considered a hybrid of a steered car and a differential drive. What generalizations are possible, and can the optimal trajectories be determined for a generic mechanism whose design is described in terms of a set of variable parameters? Which mechanism should be chosen to be most efficient for a given distribution of start and goal configurations?

9 Acknowledgments

References

[1] D. J. Balkcom and M. T. Mason. Time optimal trajectories for differential drive vehicles. *International Journal of Robotics Research*, 21(3):199–217, 2002.

[2] H. Chitsaz, S. M. LaValle, D. J. Balkcom, and M. T. Mason. Minimum wheel-rotation paths for differential-drive mobile robots. In *IEEE International Conference on Robotics and Automation*, 2006. To appear.

[3] M. Chyba and T. Haberkorn. Designing efficient trajectories for underwater vehicles using geometric control theory. In *24rd International Conference on Offshore Mechanics and Artic Engineering*, Halkidiki, Greece, 2005.

[4] A. T. Coombs and A. D. Lewis. Optimal control for a simplified hovercraft model. Preprint.

[5] G. Desaulniers. On shortest paths for a car-like robot maneuvering around obstacles. *Robotics and Autonomous Systems*, 17:139–148, 1996.

[6] L. E. Dubins. On curves of minimal length with a constraint on average curvature and with prescribed initial and terminal positions and tangents. *American Journal of Mathematics*, 79:497–516, 1957.

[7] T. Kalmár-Nagy, R. D'Andrea, and P. Ganguly. Near-optimal dynamic trajectory generation and control of an omnidirectional vehicle. *Robotics and Autonomous Systems*, 46:47–64, 2004.

[8] L. S. Pontryagin, V. G. Boltyanskii, R. V. Gamkrelidze, and E. F. Mishchenko. *The Mathematical Theory of Optimal Processes*. John Wiley, 1962.

[9] J. A. Reeds and L. A. Shepp. Optimal paths for a car that goes both forwards and backwards. *Pacific Journal of Mathematics*, 145(2):367–393, 1990.

[10] D. B. Reister and F. G. Pin. Time-optimal trajectories for mobile robots with two independently driven wheels. *International Journal of Robotics Research*, 13(1):38–54, February 1994.

[11] M. Renaud and J.-Y. Fourquet. Minimum time motion of a mobile robot with two independent acceleration-driven wheels. In *Proceedings of the 1997 IEEE International Conference on Robotics and Automation*, pages 2608–2613, 1997.

[12] I. Robert L. Williams, B. E. Carter, P. Gallina, and G. Rosati. Dynamic model with slip for wheeled omnidirectional robotos. *IEEE Transactions on Robotics and Automation*, 18(3):285–293, June 2002.

[13] P. Souères and J.-D. Boissonnat. Optimal trajectories for nonholonomic mobile robots. In J.-P. Laumond, editor, *Robot Motion Planning and Control*, pages 93–170. Springer, 1998.

[14] P. Souères and J.-P. Laumond. Shortest paths synthesis for a car-like robot. *IEEE Transactions on Automatic Control*, 41(5):672–688, May 1996.

[15] H. Sussmann. The Markov-Dubins problem with angular acceleration control. In *IEEE International Conference on Decision and Control*, pages 2639–2643, 1997.

[16] H. Sussmann and G. Tang. Shortest paths for the Reeds-Shepp car: a worked out example of the use of geometric techniques in nonlinear optimal control. SYCON 91-10, Department of Mathematics, Rutgers University, New Brunswick, NJ 08903, 1991.

[17] M. Vendittelli, J. Laumond, and C. Nissoux. Obstacle distance for car-like robots. *IEEE Transactions on Robotics and Automation*, 15(4):678–691, 1999.